Quench Localization in Superconducting Radio-Frequency Cavities

Ramesh Adhikari
Office of Science, Lee Teng Undergraduate Internship in Accelerator Science and Engineering

Berea College, Berea

Fermi National Accelerator Laboratory
Batavia, Illinois

August 9, 2010

Prepared in partial fulfillment of the requirement of the Office of Science, Department of Energy's Lee Teng Undergraduate Internship in Accelerator Science and Engineering program under the direction of Elvin Harms at Fermi National Accelerator Laboratory.

Participant: ______________________________________
Signature

Research Advisor: ______________________________________
Signature

ABSTRACT

Quench Localization in Superconducting Radio-Frequency Cavities
Ramesh Adhikari (Berea College, Berea, KY 40404), Elvin Harms (Fermi National Accelerator Laboratory, Batavia, IL 60510).

Superconducting radio-frequency (SRF) cavities are the accelerating components for the next generation of particle accelerators. Unlike the normal-conducting cavities, the SRF cavities, in principle, can stand a high electric field gradient (up to 60 MV/m for pure niobium) with very low dissipation of the RF power. Cavities that perform at the accelerating gradient of 30-35 MV/m are the current state of the art. Since the cavities installed in an accelerator must demonstrate no quenches during routine high-gradient operation, limitations to such performance must be identified and removed entirely during their manufacture and testing. Such quenches can be detected in a cold test where the cavity is kept in a superfluid helium (Helium II) bath at about 2 Kelvin and instrumented with oscillating superleak transducers (OSTs) and resistance thermal detectors (RTDs). Using the position of the transducers around the cavity and time delays for second sound signal generated by a quench to reach each of the transducers, we used a method called trilateration to calculate the location of the quench. In order to be able to perform real-time calculations for large numbers of cavities, a program based on LabVIEW was also developed. We were able to locate the quench by this method and verify our results with the complementary experimental observations obtained from RTDs.

INTRODUCTION

During the 20th century various developments in particle physics occurred, including the development of the Standard Model, discovery of quarks and neutrinos, etc. Still, some of the fundamental issues like the Higgs mechanisms and the existence of supersymmetric particles are still unknown. While the Large Hadron Collider at CERN is colliding proton-proton beams to answer the fundamental questions within the Standard Model, it is general agreement in the high-energy physics community that a lepton collider would be a complement to address these fundamental questions. Therefore, various high-energy electron-positron accelerators are under construction, including Project X at Fermilab, European XFEL, International Linear Collider, and so on. Unlike hadron accelerators, high-energy lepton accelerators cannot be circular. When the center of mass energy of the electron-positron accelerator is above 200 GeV, the synchrotron radiation loss will be significant enough that the cost of maintenance of beam energy would be drastically high [1]. Instead of this, a linear accelerator can be used to accelerate the leptons. With linear accelerators, we cannot accelerate the particles like in a circular accelerator by feeding more energy at every cycle. Instead, we have to be able to accelerate the particles as fast within a limited distance, which can be done by increasing the electric field gradient of the accelerating component. Due to the low beam impedance, ability to stand high electromagnetic field and high conversion efficiency [1] makes the superconducting cavities the best solution for the purpose. It turns out that these cavities can not only be used in linear colliders but also for all the next generation of particle accelerators. Niobium has been the default for the superconducting cavity because it is the only superconducting material which is also malleable and ductile.

Nevertheless, there is a physical limit set by the superheating field for the superconductors. The RF magnetic field at the inner surface of the superconducting resonator should stay below the superheating field, which is about $100 - 240\ mT$ for niobium. This implies that the maximum attainable accelerating gradient for the cavities we are using would be $50 - 60\ MV/m$. This field is lower in experiments due to impurities on the inner surface, field emission of electrons and multipacting [1]. Current goals for accelerating gradient for a superconducting cavity is $35\ MV/m$, which is also the set target for cavities for ILC and Fermilab Project X. This accelerating gradient is still high enough that the cavities should be virtually smooth to stand the field. If there is any physical defect in the cavity, the RF energy that is fed into the cavity for the acceleration of the particle would be absorbed around the location of defect. Niobium is a bad thermal conductor, with thermal conductivity of about $125\ Wm^{-1}K^{-1}$ ($RRR = 500$) at $4.2K$. Hence, the absorbed energy at the defect will build up upon itself and heat the surface of the cavity. As the temperature of the cavity surface increases, the cavity would not be superconducting anymore and hence would not perform as designed. Therefore, the quench detection has been a very important part of manufacturing the cavities.

Traditionally, the quenches have been located by using thermometry, which needs numbers of resistance thermal detectors (RTDs) attached on the surface of a cavity. While this method is useful to find the region where the quench has occurred in the cavity, the process is painstaking especially while working for larger projects. In this paper, we describe a method where we can use signals from oscillating superleak transducers (OSTs) to locate the exact quench spot in the cavity. We have also developed a program based on LabVIEW, which will make the process much more efficient than the traditional approach.

MATERIALS AND METHODS

Oscillating Superleak Transducers (OSTs)

A quench on a cavity dissipates the input RF energy in the form of heat, which will be transmitted to its surrounding by diffusion. If there is superfluid helium (He II) as the surrounding, then the heat is transmitted in the form of a wave instead of diffusion, as first observed by Peshkov in 1944A.D. This thermal wave is analogous to sound wave and referred to as second sound wave. Velocity of this wave is dependent on the temperature of superfluid. A second sound wave can be detected by using an electrostatic transducer, commonly called an OST.

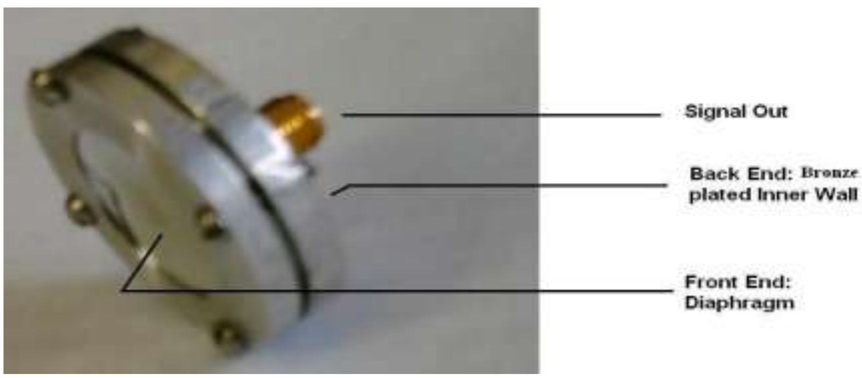

Figure 1: Oscillating superleak transducer (OST).

OSTs are cylindrical in structure. One end of the cylinder is closed by a diaphragm which, in our case, is a polycarbonate fiber with 0.2 μm pores coded with 0.5 nm of aluminum. On the other end of the cylinder, opposite the diaphragm, a bronze layer of thickness of 0.02 mm is coated on the aluminum wall and is connected to an SMA connector. At this end, second sound signal is converted into electrical signal and transmitted to an oscilloscope, taking advantage of the capacitor-like interaction between the diaphragm and the bronze-coated wall.

OSTs are appealing due to their efficiency of operation. Efficiency of such a transducer can be written as:

$$\frac{E_2}{E_1} = \frac{\rho_s}{\rho_n} \tag{1}$$

where, E_1 and E_2 is the energy density of the second sound while ρ_s and ρ_n are the mass densities of the normal and superfluid component of He II. For He II, the density of normal fluid is given as [7]:

$$\rho_s = \rho.\left[1 - \left(\frac{T}{T_\lambda}\right)^{5.6}\right] \tag{2}$$

where, T is the temperature and T_λ is the λ point of the superfluid. As we can see, the superfluid density increases with decreasing temperature. For such case, we can see that the energy density for second sound in OST is larger than for the first sound and hence more efficient than other kind of transducers like the Peshkov transducer [6].

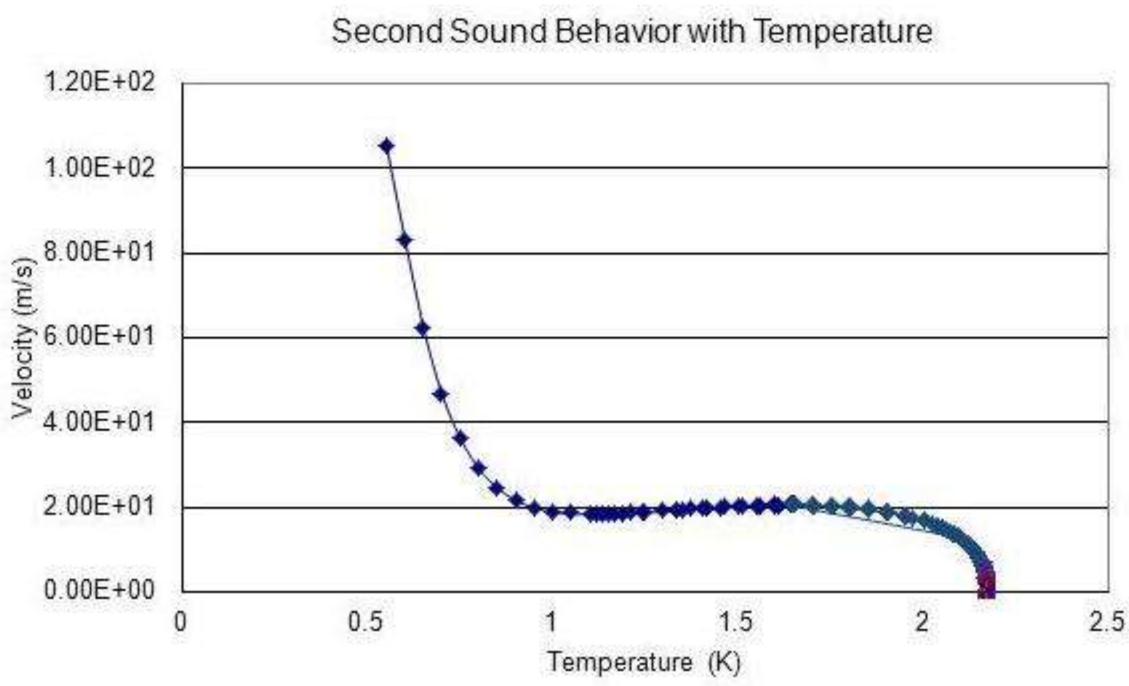

Figure 2: Velocity response of second sound with temperature.

Occurrence of quench can be observed as sudden drop in RF energy coming out of the cavity. When the second sound reaches a transducer, we can also observe an abrupt decrement in its output voltage. If there are three or more OSTs around the cavity, then various time delays are detected. One can measure the time delays between the quench occurrence and the signals detection by the OSTs. From various other experiments, we know the velocity of the second sound at different temperatures. Then, we can learn about the distance of the quench from each detector. Using a method called trilateration, we can compute the location of the quench.

Trilateration

Let's imagine that the OSTs are located at the center of the spheres of radii, which are equivalent to distances between the quench location and themselves. We already described the method of getting the distances between OSTs and quench. Now, we can think of all these spheres intersecting with each other at the quench location. For practical reasons, the center of the cavity can be considered to be the origin of the 3D coordinate system that would define the position of all the OSTs and also the quench.

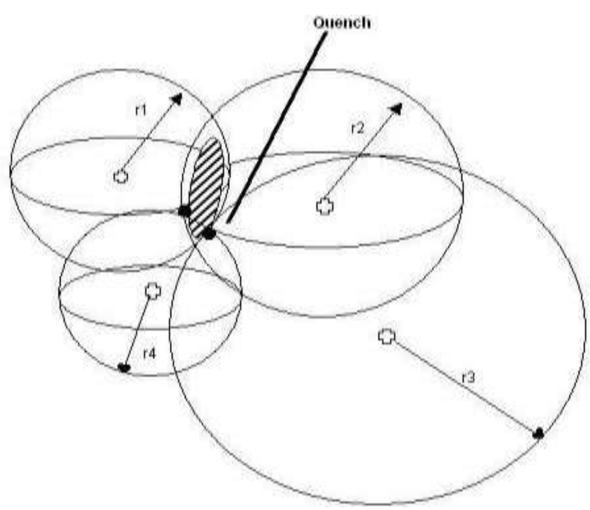

Figure 3: Trilateration: Visualization of location of quench.

For this method, we will need four OSTs to exactly locate the quench. Suppose the location of the OSTs are x, y, z, where i = 1, 2, 3, 4 for four OSTs and quench be located at x, y, z. Then, the distance between OST and quench would be:

$$(x_i - x)^2 + (y_i - y)^2 + (z_i - z)^2 = r_i^2 \tag{3}$$

Hence, the distance of each OST from the quench will be:

for i = 1,

$$(x_1 - x)^2 + (y_1 - y)^2 + (z_1 - z)^2 = r_1^2 \tag{4}$$

for i = 2,

$$(x_2 - x)^2 + (y_2 - y)^2 + (z_2 - z)^2 = r_2^2 \tag{5}$$

for i = 3,

$$(x_3 - x)^2 + (y_3 - y)^2 + (z_3 - z)^2 = r_3^2 \tag{6}$$

for i = 4,

$$(x_4 - x)^2 + (y_4 - y)^2 + (z_4 - z)^2 = r_4^2 \tag{7}$$

We can subtract (4) from (5), (6) and (7) and get rid of nonlinear terms. Then we arrange the left-over terms in a matrix form as:

$$M = \begin{matrix} 2(x_2 - x_1) & 2(y_2 - y_1) & 2(z_2 - z_1) & s \\ 2(x_3 - x_1) & 2(y_3 - y_1) & 2(z_3 - z_1) & t \\ 2(x_4 - x_1) & 2(y_4 - y_1) & 2(z_4 - z_1) & u \end{matrix} \tag{8}$$

where,

$$s = x_2^2 - x_1^2 + y_2^2 - y_1^2 + z_2^2 - z_1^2 - r_2^2 - r_1^2 \tag{9}$$

$$t = x_3^2 - x_1^2 + y_3^2 - y_1^2 + z_3^2 - z_1^2 - r_3^2 - r_1^2$$

$$u = x_4^2 - x_1^2 + y_4^2 - y_1^2 + z_4^2 - z_1^2 - r_4^2 - r_1^2$$

We know that the solution of linear equations in this form of matrix can be obtained from reduced row echelon form of the augmented matrix above. This reduced row echelon form of the matrix can be found by Gaussian elimination. For the acknowledgment of the row echelon form of a matrix, suppose the above matrix can be written as:

$$E = \begin{matrix} 1 & 0 & 0 & a \\ 0 & 1 & 0 & b \\ 0 & 0 & 1 & c \end{matrix} \quad (10)$$

Here, a, b and c can be easily calculated provided that we have the information about (x_1, y_1, z_1), (x_2, y_2, z_2), (x_3, y_3, z_3) and (x_4, y_4, z_4) which are basically the position of the transducers with respect to the center of the cavity and r_1 , r_2 and r_3 which are the distance of the quench from each transducer. The position of the quench (x, y, z) can be calculated as:

$$x = a, \qquad y = b, \qquad z = c \quad (11)$$

Based on this mathematical principle, we developed a program based on LabVIEW that would intake the parameters like coordinates of the transducers, velocity of second sound wave, and time delay of the second sound signal on each of the four transducers and compute the reduced row echelon form of the generated matrix. Finally, the program would output the quench location in 3D space. The simulated cavity image and the quench location will be displayed as shown in Figure 9.

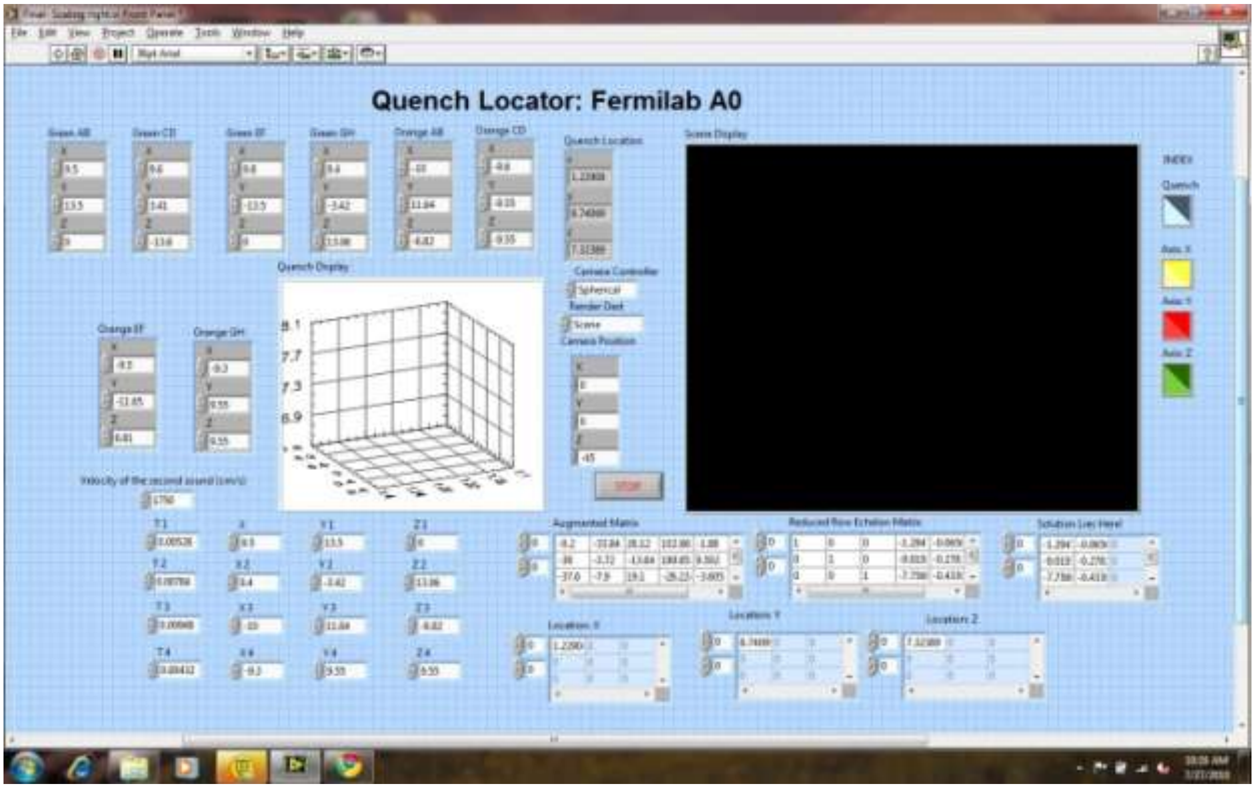

Figure 4: Screenshot of the developed user interface for entering data.

RESULTS

The experiment is performed at the temperature on or below 2 K. A cold test is set up as shown in the figure (5). A cavity is kept in equipment made up of four bars that hold two plastic circular discs on their either ends. The center of the cavity is arranged to be at the midpoint between two circular plastic discs. On each of these discs, four OSTs are attached. The setup is kept vertically such that four of these OSTs are on the bottom region of the cavity and four on the top. Each of the OSTs is marked AB, CD, EF or GH. The OSTs on the bottom region are called orange; OSTs on the top regions are called greens and are rotated by an angle of 45° counterclockwise.

We assume that the center of the cavity will be the origin of the coordinate which we will use to define the position of OSTs, RTDs and quench. Using some geometry and the law of cosines, we define the coordinates of the transducers as $(9.5, 13.5, 0)$, $(9.6, 3.41, -13.6)$, $(9.8, -13.5, 0)$ and $(9.4, -3.42, 13.06)$ for green AD, CD, EF and GH respectively. Similarly, the positions of the orange transducer were defined as $(-9.3, 9.55, 9.55)$, $(-10, 11.64, -6.82)$, $(-9.6, -9.55, -9.55)$ and $(-9.5, -11.65, 6.81)$ for GH, AB, CD and EF respectively. It needs to be noted that for this system a unit is a centimeter.

Figure 5: A cold test setup. A niobium cavity is surrounded by numbered RTDs around its equatorial region. Alphabetical numberings(e.g. GH, EF) are for OSTs.

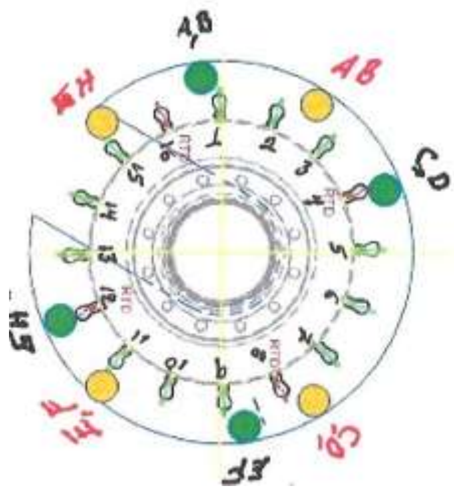

Figure 6: Top view of the arrangement of the OSTs during the cold test.

Such arrangement of the OSTs is to maximize the exposed area for the OSTs. This will allow us to lower the probability that we will miss any quench location on the cavity. Also, to find complementary data to verify the quench location, 16 RTDs are attached around the equator of the cavity. This will allow us to have an idea of the location of the quench because we know that the quench should be around the region where the RTDs with maximum temperature gradient are located.

Observation

The quench activity is monitored on a oscilloscope that reads data from RF energy and three transducers. The blue line represents the RF field. We can also see the readings from the transducers as shown in magenta, cyan and green as in figures 7 and 8. Initially, the voltage signal is leveled. As the second sound reaches the diaphragm of a OST, it starts to vibrate with the normal fluid while the second sound passes freely. Hence, the capacitance of the transducer fluctuates during the event, which we can see on the oscilloscope as a quench. As we are interested on the first disturbance, which is due to first arrival of the second sound, we can measure the time delay between actual quench occurrence and arrival of the second sound at the transducers.

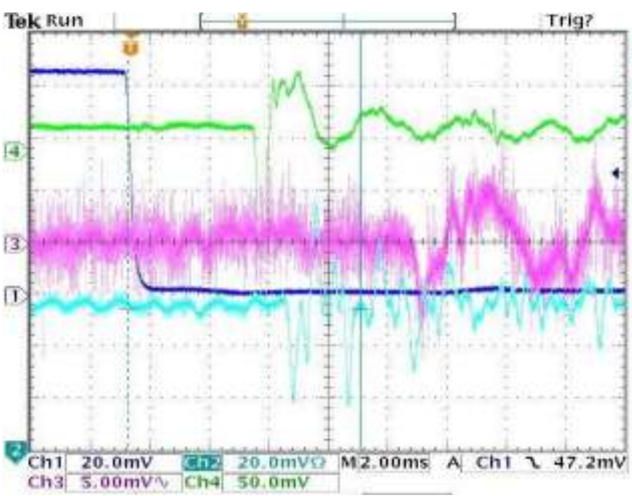

Figure 7: A screenshot of the reading from oscilloscope which reads information from RF signal and three transducers. Channel 2 (cyan) corresponds to green AB, channel 3 (magenta) corresponds to orange AB and channel 4 (green) corresponds to orange GH. Channel 1 (blue) represents the RF signal.

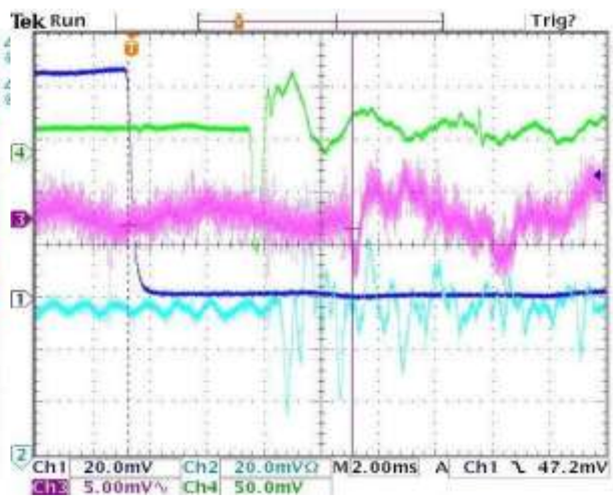

Figure 8: A screenshot of the reading from oscilloscope which reads information from RF signal and three transducers. Channel 2 (cyan) corresponds to green AB, channel 3 (magenta) corresponds to green GH and channel 4 (green) corresponds to orange GH. Channel 1 (blue) represents the RF signal.

In this case, the quench occurred at the gradient of about 33.7 MV/m. We observed that the time delay for second sound readings for green AB, green GH, orange AB, and orange GH are 5.28 ms , 7.48 ms, 9.48 ms and 4.32 ms respectively. The reading was taken at the temperature $1.7K$. The velocity of the second sound at this temperature of He II is $17.5m/s$. We can easily calculate the distance of the quench from the three transducers as 9.24 cm, 13.72 cm, 16.59 cm and $7.56cm$ respectively. Now we can enter the locations of the three transducers in a coordinate system in which the center of the cavity is the origin and then find the quench location by the algorithm explained in the earlier section. Our calculation for this case shows that the quench should be located on the cavity at the point $(1.229, 8.741, 7.324)$ in centimeters and is displayed on the cavity as shown in Figure 9.

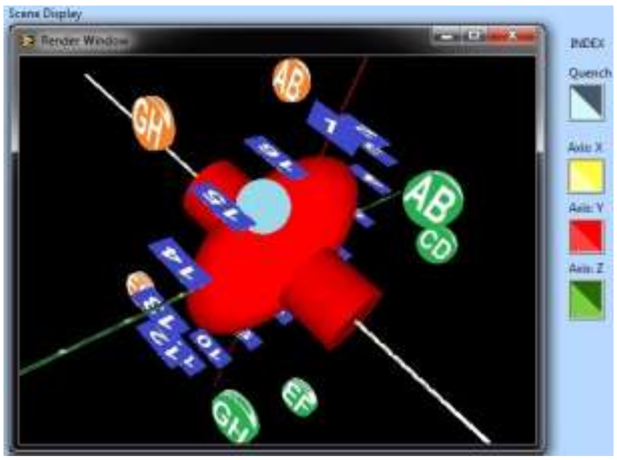

Figure 9: Screenshot of a computer 3D display of the quench on the cavity. Green and orange transducers and RTDs (in blue) are shown for reference.

Verification

For this experiment, the temperature gradient was observed on RTDs 14, 15 and 16. Now we can refer to the map of the cavity at Figure 6 and locate the region in the cavity that should have the quench. We can affirm that the quench should be located on the area that is closer to the above-stated RTDs. This is exactly the expected location based on the calculation using trilateration. Now one can perform optical testing and then clean up the defect with electropolishing or any other technique.

CONCLUSION

We were able to locate the quench on the cavity and our finding was consistent with the readings from RTDs. LabVIEW was also effective to perform the expected computation and displays. Also, the quantitative study of the effectiveness of the algorithm can be performed by optical tests and getting the actual location of the quench and compare it with the computed location. Another step from this project can be performing 9-cell cavity tests using OSTs to further speedup the process. Nevertheless, there might be some complexities in such tests due to the cases like multiple quenching. But, it is encouraged that such tests shall be carried out and further studied.

It also needs to be pointed out that the algorithm we developed requires a response from four OSTs. If we can devise some equation that provides the cavity geometry, then we might be able to lower the number of OSTs required to two for the location of the quench. For the next phase, using MATLab might be a better option, which allows a programmer to perform numerical analysis and approximations based on the geometry of the cavity, location of OSTs and distance between quench and OSTs.

ACKNOWLEDGEMENTS

I would like thank my mentor, Elvin Harms, whose advice, support and direction made this project complete. I would also like to thank Helen Edwards and other staff members of the Fermilab A0-Photoinjector facility who were always ready to help in need and made my early week in transition easy. Also, I would like to thank Eric Prebys and Linda Spentzouris for managing the internship and arranging various programs that were an integral part of learning during the internship. I would like to thank Lee Teng and DOE for making this internship possible. I would also like to thank Carol Angarola for putting everything together and helping out with paperwork, housing, etc. and also LaMargo Gill for assisting with this paper. I would also like to thank Eric Ramberg and Roger Dixon for their Wednesday meeting sessions that were full of exciting discussions on particle physics. Also, I would like to thanks fellow Lee Teng, SULI and PST students for making the internship duration memorable.

REFERENCES

[1] B. Aune, R. Bandelmann, D. Bloess, et al., "Superconducting TESLA cavities," *Physical Review Special Topics — Accelerators and Beams*, vol 3, 092001-1, 25 pages, 2000.

[2] Z.A. Conway, C.P. Hartill, H.S. Padamsee, and E.N.Smith, "Defect location in superconducting cavities cooled with He-II using oscillating superleak transducers," Cornell University, Ithaca, NY.

[3] J.C. Han, B.J. Park, W.Y. Lee, H. Han, Y.J. Kim, S.B. Kim, C.S. Kim and B.W. Lee, "Photoacoustic effect at second-order phase transition in $La_{1-x}Ca_xMnO_3$, *Journal of Magnetism and Magnetic Materials*, vol. 242, pp. 716-718, 2002.

[4] D.R. Tilley and J. Tilley, "Helium II: The two-fluid model," *Graduate Students Series in Physics*, Institute of Physics Publishing, 2003.

[5] Google Books, "New effect observed in liquid helium," *New Scientist*, vol. 14, no. 285, p. 238, 1962.

[6] R.A. Sherlock and D.O. Edwards, "Oscillating superleak second sound transducers," *Review of Scientific Instruments*, vol. 41, no. 11, pp. 1603-1609, 1970 (current version 2009).

[7] S. Yuan, Superuid helium, http://www.yutopian.com/Yuan/HeII.html.

[8] E. W. Weisstein, Gaussian elemination, http://mathworld.wolfram.com/GaussianElimination.html.